Performance Study of Scraped Surface Heat Exchanger with Helical Ribbons

S. Ali, M. Baccar

Abstract—In this work, numerical simulations were carried out using a specific CFD code in order to study the performance of an innovative Scraped Surface Heat Exchanger (SSHE) with helical ribbons for Bingham fluids (threshold fluids). The resolution of three-dimensional form of the conservation equations (continuity, momentum and energy equations) was carried out basing on the finite volume method (FVM). After studying the effect of dimensionless numbers (axial Reynolds, rotational Reynolds and Oldroyd numbers) on the hydrodynamic and thermal behaviors within SSHE, a parametric study was developed, by varying the width of the helical ribbon, the clearance between the stator wall and the tip of the ribbon and the number of turns of the helical ribbon, in order to improve the heat transfer inside the exchanger. The effect of these geometrical numbers on the hydrodynamic and thermal behaviors was discussed.

Keywords—Heat transfer, helical ribbons, hydrodynamic behavior, parametric study, scraped surface heat exchanger, thermal behavior.

I. INTRODUCTION

SSHE are used in food and chemical industries for several thermal applications such as multiphase fluid systems, freezing, heating and cooling viscous products, etc. Back mixing and fouling are two major problems in processing viscous and sticky products. They cause a reduced overall heat transfer coefficient which means decrease the performance of the exchanger. One of the several solutions is replacing the rotating blades found in the commercial practices by helical ribbon. Studying heat transfer within SSHE was the interest of many researchers; De Goede and De Jong [1] studied the development of a vortex between the scraper blades in the turbulent regime using a CFD model and he finished by developing a theoretical model to predict thermal performance. Baccar and Abid [2] did a 3D numerical simulation in order to analyse the hydrodynamic and thermal behaviour under different geometrical and operating conditions. M. Örvös et al. [3] gave an experimental study in order to determine a heat transfer equation by varying different operational parameters. Ben Lakhdar et al. [4] established the influence of many parameters (product type and composition, blade rotation speed, flow rate and distance between blades and wall) on heat transfer. They carried out an experimental study on SSHE used for freezing of water-ethanol mixture and aqueous sucrose solution and they found two correlations one for the ethanol and the other for the sucrose. Martinez et al. [5] created an innovative heat exchanger which is mechanically assisted by a reciprocating cylinder, they analysed the flow pattern and pressure drop mechanisms in static and dynamic conditions. Yataghene et al. [6] achieved a 3D-numerical modelling to examine the thermal performance of a SSHE for Newtonian and non-Newtonian fluids with varying blades speed and mass flow rate. Boccardi et al. [7] developed two heat transfer correlations for a SSHE using experimental data, they used for the first one the dimensionless geometrical number D/L, and for the second one a new number which considers other agitator characteristics. In a previous work [8], we have determined the influence of dimensionless numbers (axial Reynolds and rotational Reynolds numbers and Oldroyd number) on the hydrodynamic and thermal behaviors.

SSHE consists of:
- stator which is the heat exchanger surface with the fluid,
- rotor which contains rotating blades, it rotates continuously in order to prevent the crust formation by scraping the exchanger surface.

This study presents an innovative SSHE which, instead of using scraping blades, is assisted by helical ribbon (see Fig. 1). Three-dimensional numerical simulations of threshold fluids are performed in order to understand the influence of the clearance between the tip of the ribbon and the exchanger wall, the ribbon's width and the number of turns on hydrodynamic and thermal behaviors within SSHE with helical ribbons.

S. Ali is with Research Unit of Computational Fluid Dynamics and Transfer Phenomena (CFDTP) – Mechanical Engineering Department, the National Engineering School of Sfax, Soukra Street Km3.5, Bp 1173, 3038 Sfax, Tunisia (phone: 0021653445658; e-mail: sirineali@ymail.com).

M. Baccar is with Research Unit of CFDTP – Mechanical Engineering Department, National Engineering School of Sfax (ENIS), Soukra Street Km3.5, Bp 1173, 3038 Sfax, Tunisia (e-mail: mounir.baccar@enis.rnu.tn).
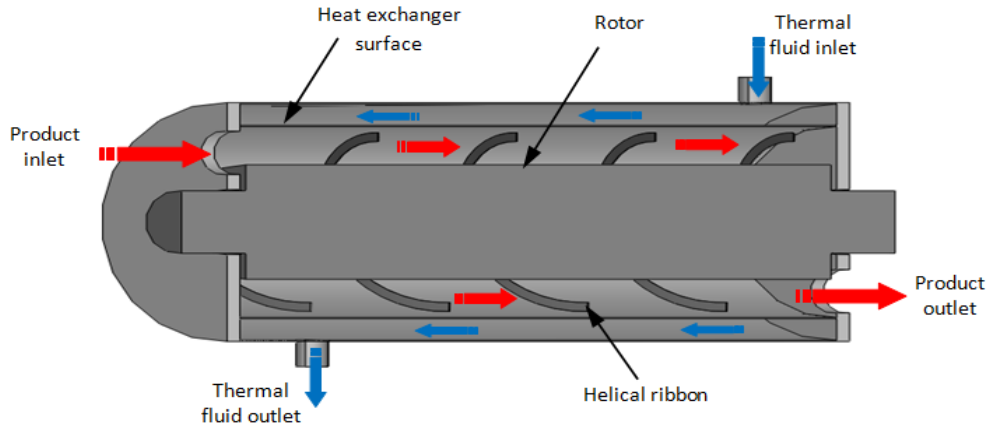
II. NUMERICAL MODEL

A. Geometry and Mesh

A specific CFD (Computational Fluid Dynamics) code was used in the simulation of the hydrodynamic and thermal behaviors. The methods of discretization used for the modeling of velocity and temperature fields were the hybrid scheme and the exponential scheme, respectively. The ratio of rotor shaft radius to internal exchanger radius (r/R) is equal to 0.6. The ratio of exchanger height to its internal radius (H/R) is equal to 6. This configuration is the same as that studied experimentally by [9] and numerically by [2].

The helical ribbon extends over four pitches (see Fig. 1). It was driven by the rotor, to continuously scrape the stator wall.

The grid size used in the simulation is 230400 computational cells (36 in the radial, 40 in the tangential and 160 in the axial direction).

Fig. 1 Scheme of the SSHE model

TABLE I
NOMENCLATURE

Symbol	Quantity	SI Units
C_p	Specific heat of the fluid	[J/kgK]
D	Internal diameter of the exchanger	[m]
d_a	Agitator diameter	[m]
d_r	Rotor shaft diameter	[m]
h	Heat transfer coefficient	[W/m²K]
L	Length of the exchanger	[m]
N	Rotational speed	[rev/s]
P	Pressure	[Pa]
p	Pitch of the helical ribbon	[-]
R	Internal exchanger radius	[m]
r	Rotor shaft radius	[m]
T	Temperature	[K]
U,V,W	dimensionless velocity components	[-]
r,θ,z	dimensionless coordinates system	[-]
ρ	Fluid density	[Kg/m³]
λ	Thermal conductivity of air	[W/mK]
μ	Dynamic viscosity	[Pa.s]
η	Apparent viscosity	[-]
ν	Kinematic viscosity	[m²\s]
θ	Dimensionless temperature	[-]

B. Governing Equations

In this section the conservation equations of continuity, momentum and energy have been solved basing on the FVM. The flow is considered steady, laminar, non-isothermal, and incompressible.

The continuity equation for the velocity in the rotating reference frame is written as:

$$\text{div } \vec{V} = 0 \tag{1}$$

with $\vec{V}$ is the velocity vector.

The momentum equation can be expressed in the tensorial form as:

$$\rho\left(\frac{\partial \vec{V}}{\partial t} + \overrightarrow{\text{grad}}\vec{V}.\vec{V}\right) = -\overrightarrow{\text{grad}}P + \text{div}\overline{\overline{\tau}} + \rho\vec{g} \tag{2}$$

The tensorial strain can be written considering a purely viscous generalized Newtonian fluid:

$$\overline{\overline{\tau}} = \eta\,|\dot{\gamma}| \tag{3}$$

where $\dot{\gamma}$ is the shear rate.

In a rotating frame, Centrifugal and Coriolis acceleration which defined respectively as $-w^2.\vec{r}$ and $2\vec{w}\wedge\vec{r}$ were added to the momentum equation.

The conservation equation of energy is expressed as:

$$\rho C_p \frac{\partial T}{\partial t} = -\text{div}\left(-\lambda\overrightarrow{\text{grad}}T + \rho C_p \vec{V}T\right) \tag{4}$$

C. Boundary Conditions

The mean velocity at the inlet of the exchanger is given in the dimensionless form as:

$$W_{inlet} = \frac{1}{\pi}\frac{\text{Re}_a}{\text{Re}_r}\left(\frac{d}{D}\right)^2\frac{1}{1-\dfrac{R_{rot}}{R}} \tag{5}$$

In the region where the fluid exits the computational domain, the velocity gradient equals to zero:

$$\frac{\partial W_{outlet}}{\partial z} = 0 \tag{6}$$

The presence of the rotor and helical ribbon was taken into account. Thus, all radial and tangential velocity mesh nodes which intersect with the rotor or the ribbon were taken equal to zero. The angular velocity component, at the internal wall exchanger, equal to the rotating speed because of the rotating frame. Thus, the dimensionless angular velocity is imposed equals to -1.

The boundary conditions of the temperature field are taken as follows: The temperature at the entrance of the exchanger is constant that's why the dimensionless temperature equals to zero. At the outlet of the exchanger and across the rotor the heat flux is zero (adiabatic wall). The dimensionless wall

temperature equals to 1, and the derivative of dimensionless temperature relative to z equals to 0.

$$\theta_{in} = 0$$
$$\theta_w = 1$$
$$\frac{\partial \theta}{\partial z} = 0 \qquad\qquad (7)$$

D. Rheological Model

High viscous and non-Newtonian products were treated in SSHEs. For solving momentum equation, there are many mathematical models that describe the rheological behavior, where the apparent viscosity (η) is a non-linear function of the shear rate (γ). Many of fluid materials have a yield stress, a critical value of stress below which they do not flow; they are called viscoplastic materials or Bingham plastics.

In this study, the model of Papanastasiou was considered who suggested an exponential regularization of the Bingham model, by introducing a parameter m, which controls the exponential growth of stress [10].

The proposed model, called also Bingham-Papanastasiou model, has the following form:

$$\eta = 1 + \frac{Od\left[1 - \exp\left(-m\,|\dot\gamma|\right)\right]}{|\dot\gamma|} \qquad (8)$$

The viscoplastic character of the flow is assessed by a Bingham number (Bn) or Oldroyd number (Od), defined by:

$$Bn = Od = \frac{\tau_y D}{\mu V_a} \qquad\qquad (9)$$

where τ_y is the yield stress and V_a is the average velocity of the viscoplastic fluid.

In the case of Bn = Od= 0, the fluid is Newtonian. However, at the other extreme (Bn = Od tends to infinity) the fluid is unyielded solid.

III. RESULTS AND DISCUSSION

A. Effect of the Clearance

The effect of the clearance (δ/R) between the stator wall and the tip of the ribbon on the hydrodynamic and thermal behaviors was described in this paragraph. Results are represented in (r-z) vertical mid-plane.

1. Effect on the Hydrodynamic Behavior

Fig. 2 represents the impact of the clearance (e=δ/R) on the hydrodynamic behavior. The first three cases in the figure show that when the ribbon is near to the exchanger's surface, the penetration of fluid is towards the interior of the domain. However, when e=0.1176 or e=0.1764, the ribbon is in the middle of the exchanger and the fluid is around the ribbon: a current of material is deviated towards the interior and a current is deviated towards the outside.

2. Effect on the Thermal Behavior

The representation of the thermal behavior shows that there is an optimum value below which the heat transfer increases until reaching this value, and above which the heat transfer decreases (Fig. 3).

B. Effect of the Width of the Ribbon

This paragraph includes the impact of the ribbon's width (W/R) on both hydrodynamic and thermal behaviors in (r-z) vertical mid-plane.

1. Effect on the Hydrodynamic Behavior

Fig. 4 shows that when decreasing the width of the ribbon, the recirculation zones decreases because the fluid materials surround the helical ribbon.

2. Effect on the Thermal Behavior

The representation of the thermal behavior shows that the highest values of temperature were next to the exchanger's wall and around the helical ribbon that is why the heat transfer decreases when decreasing the width of the ribbon (Fig. 5).

In Fig. 5, the impact of the clearance and the ribbon's width on the Nusselt number was studied. Numerical results show that the highest value of heat transfer coefficient is when the clearance equals to e=δ/R=0,0702 (optimum value) for different cases of the ribbon's width.

C. Effect of the Number of Turns in the Ribbon

This paragraph contains examples of the numerical results giving the velocity and temperature fields in (r-z) vertical mid-plane in order to study the effect of the number of turns in the helical ribbon.

1. Effect on the Hydrodynamic Behavior

Fig. 7 shows the effect of the number of turns in the ribbon on the hydrodynamic behavior for two cases: when the ratio of rotational Reynolds to axial Reynolds is inferior than 1 (r<1) and when it is superior than 1 (r>1). When increasing the number of turns (from 4 turns to 6 turns) the back-mixing phenomenon is near to disappear.

2. Effect on the Thermal Behavior

The representation of the thermal behavior shows that there is an optimum value below which the heat transfer increases until reaching this value, and above which the heat transfer decreases (Fig. 8) reproduces temperature distribution for two number of turns (4 and 6 turns). It appears that the increase of the number of turns in the ribbon produces a rise in the temperature field. That is to say that increasing the number of turns in the ribbon leads to ameliorate the heat transfer within the exchanger.
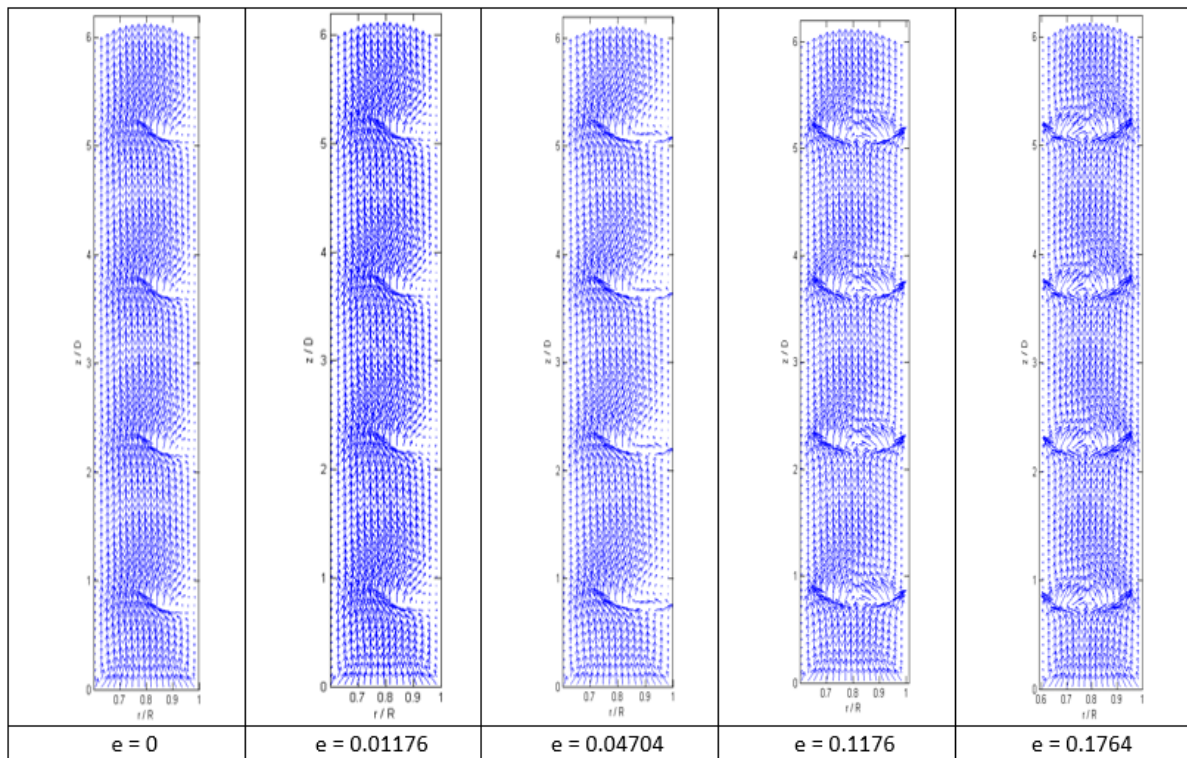
| e = 0 | e = 0.01176 | e = 0.04704 | e = 0.1176 | e = 0.1764 |

Fig. 2 Effect of the clearance on the hydrodynamic behavior

| e = 0 | e = 0.01176 | e = 0.04704 | e = 0.1176 | e = 0.1764 |
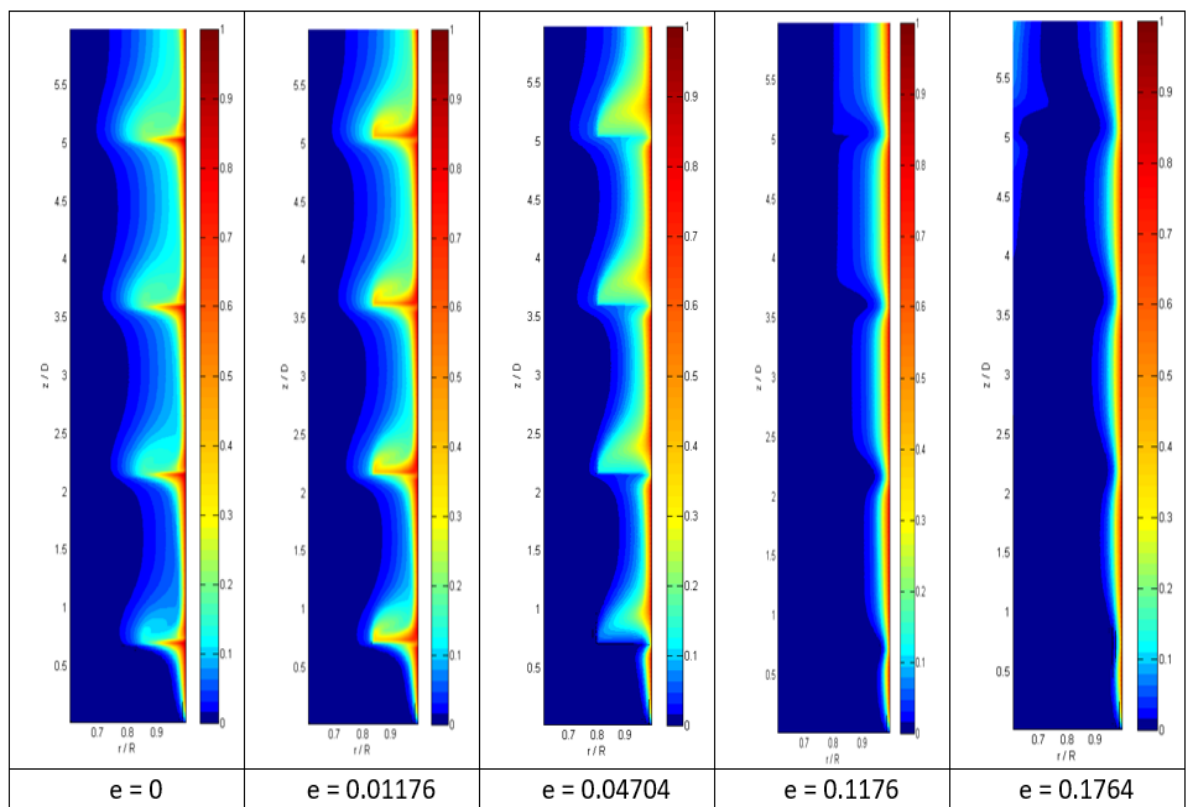
Fig. 3 Effect of the clearance on the thermal behavior

W / R = 0.15	W / R = 0.129	W / R = 0.105	W / R = 0.08
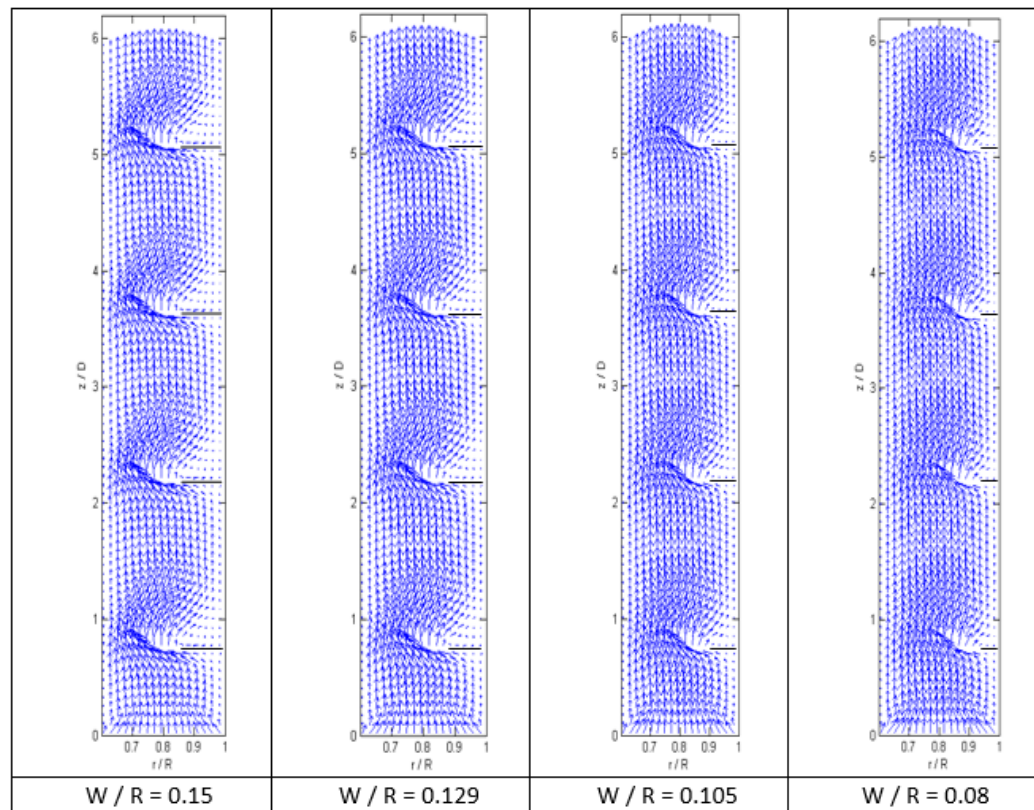
Fig. 4 Effect of the ribbon's width on the hydrodynamic behavior

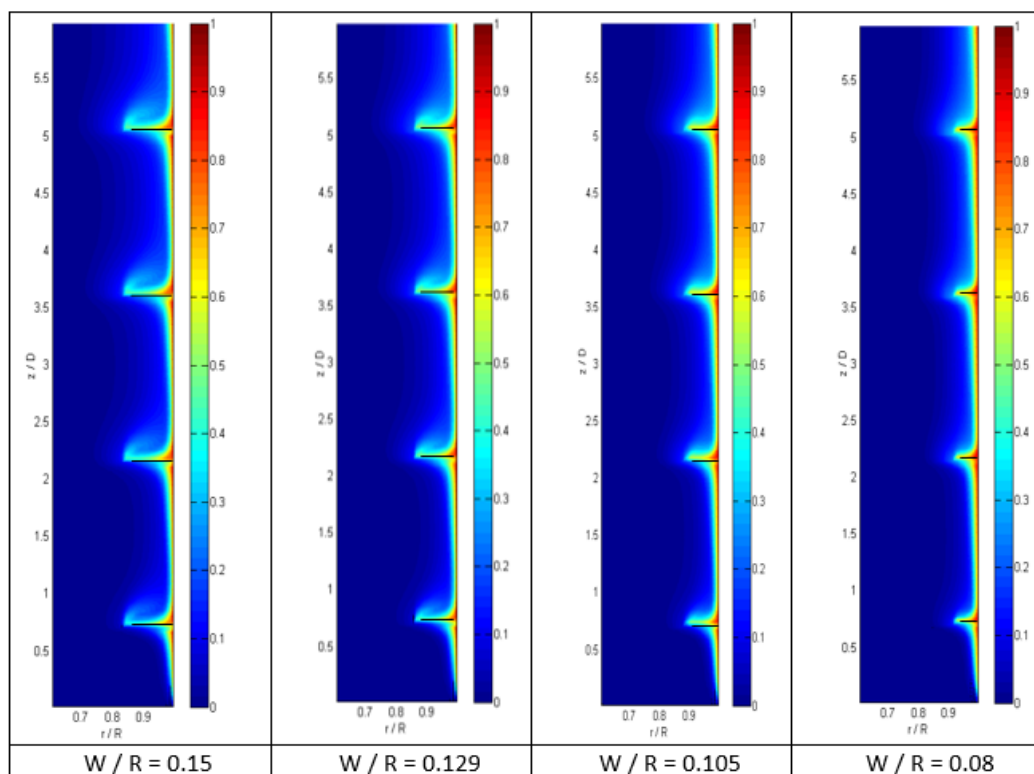|			
W / R = 0.15	W / R = 0.129	W / R = 0.105	W / R = 0.08

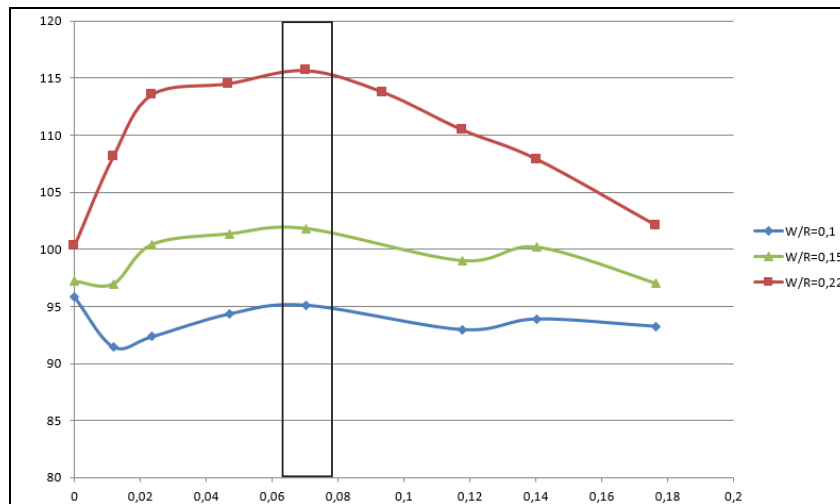Fig. 5 Effect of the ribbon's width on the thermal behavior

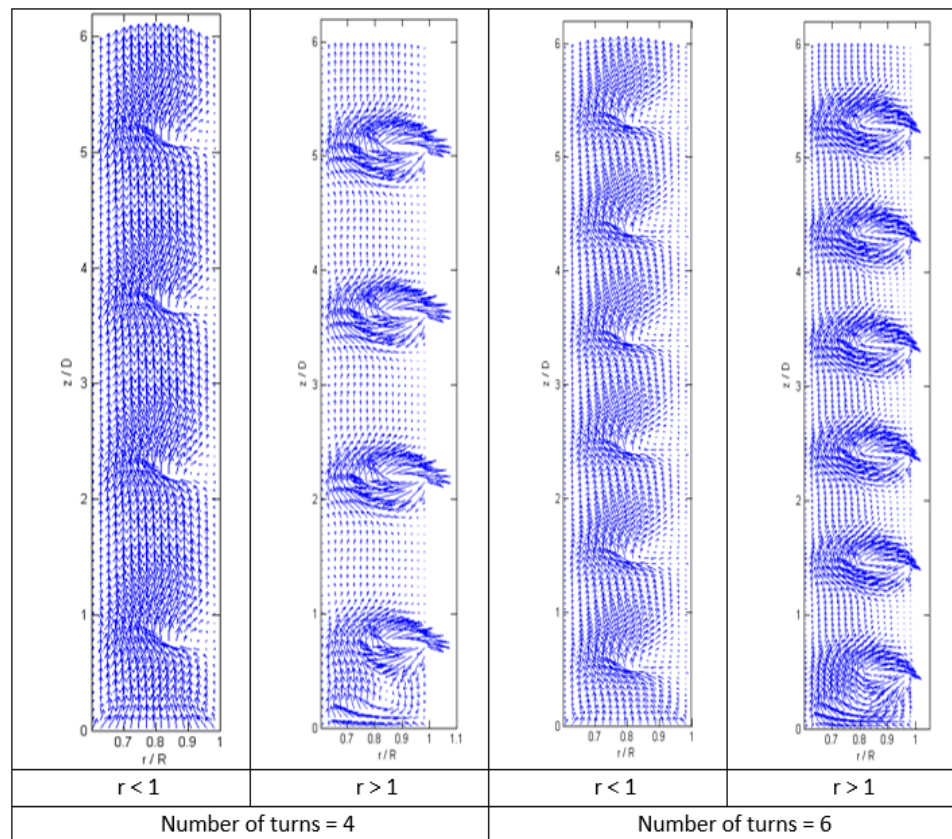Fig. 6 Nusselt as a function of the clearance and the ribbon's width

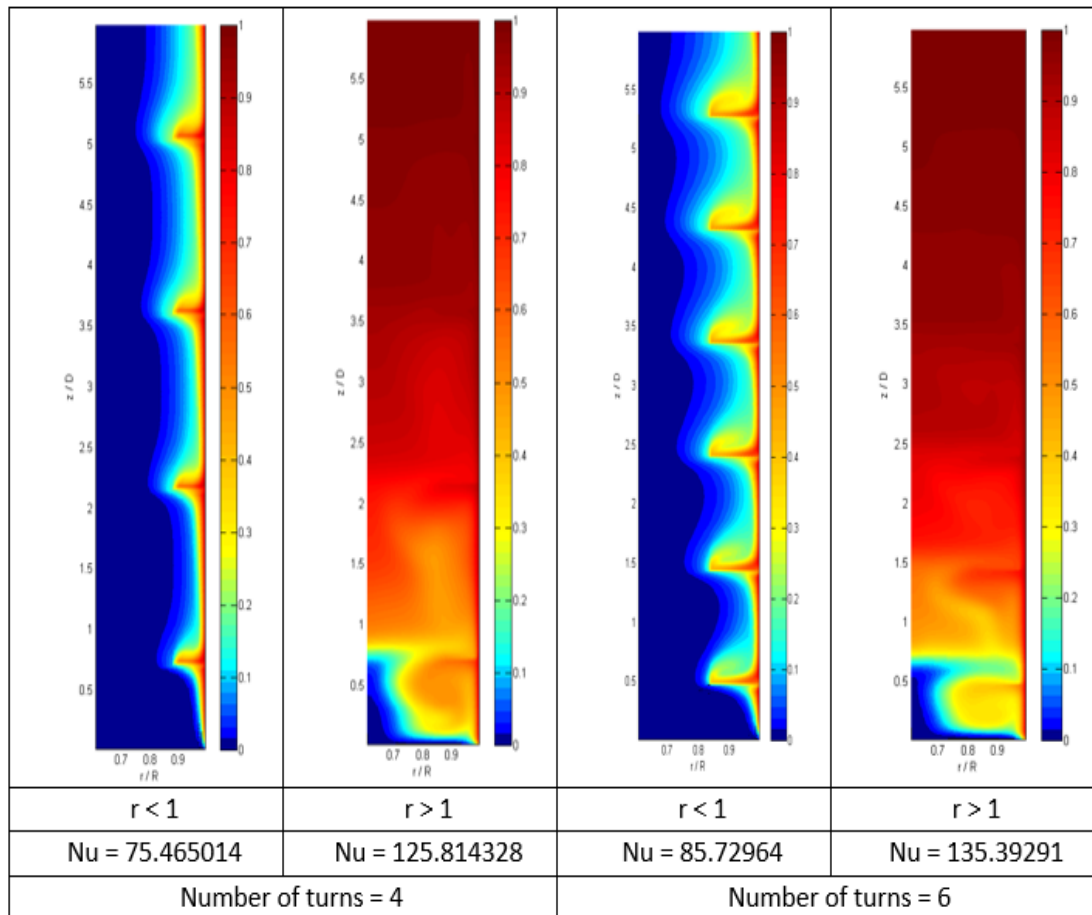Fig. 7 Effect of the number of turns on the hydrodynamic behavior

r < 1	r > 1	r < 1	r > 1
Nu = 75.465014	Nu = 125.814328	Nu = 85.72964	Nu = 135.39291
Number of turns = 4		Number of turns = 6	

Fig. 8 Effect of the number of turns on the thermal behavior

IV. CONCLUSION

The aim of this work is to study the impact of the geometric parameters (the clearance, the ribbon's width, and the number of spires) on the hydrodynamic and thermal behavior. We found that the heat transfer increases when increasing the width of the ribbon and that there is an optimum value of the clearance between the tip of the ribbon and the exchanger wall which is equal to 0,0702. We found also that when the number of turns gets bigger, the heat transfer increases and the back-mixing phenomenon is near to disappear.

A heat transfer correlation using dimensionless and geometric numbers will be given afterwards in order to predict the heat transfer coefficient.

REFERENCES

[1] R. De Goede, E.J. De Jong, Heat transfer properties of scraped-surface heat exchanger in the turbulent flow regime, Chem. Eng. Sci. 48 (1993) 1393-1404.
[2] M. Baccar, M.S. Abid, Numerical analysis of three-dimensional flow and thermal behavior in a scraped-surface heat exchanger, Rev. Gen. Therm. 36 (1997) 782-790.
[3] M. Örvös, T. Balazs, K.F. Both, and I. Csury, Investigation of heat transfer conditions in scraped surface heat exchanger, Periodica Polytechnica Ser. Mech. Eng. 98 (1994) 129-198.
[4] M. Ben Lakhdar, R. Cerecero, G. Alvarez, J. Guilpart, D. Filck, and A. Lallemand, Heat transfer with freezing in a scraped surface heat exchanger, Applied Thermal Engineering 25 (2005) 45-60.
[5] D. S. Martinez, J.P. Solano, J. Pérez, A. Viedma, Numerical investigation of non-Newtonian flow and heat transfer in tubes of heat exchangers with reciprocating insert devices, Frontiers in Heat and Mass Transfer, 2, 033002, DOI: 10.5098. v2.3.3002 (2011).
[6] M. Yataghene, J. Legrand, A 3D-CFD model thermal analysis within a scraped surface heat exchanger, Computer & Fluids 71 (2013) 380-399.
[7] G. Boccardi, G.P. Celata, R. Lazzarini, R. Saraceno, and R. Trinchieri, Development of a heat transfer correlation for a scraped-surface heat exchanger, Applied Thermal Engineering 30 (2010) 1101-1106.
[8] S. Ali, M. Baccar, Numerical study of hydrodynamic and thermal behaviors in a scraped surface heat exchanger with helical ribbons, Applied Thermal Engineering 111 (2017) 1069-1082.
[9] A. M. Trommelen, W.J. Beek, Flow phenomena in scraped-surface heat exchanger, Chem. Eng. Sci. 26 (1971) 1933-1942.
[10] E. Mitsoulis, Flows of viscoplastic materials: models and computations, Rheology Reviews (2007) 135-178.